

Investigation of Synergistic Inhibition Effect of Methyl Violet and Bromide on the Corrosion of Mild Steel in Phosphoric Acid Solution

Lin Wang^{*}, Meng-Qiao Qu, Yan-Ju Yang, Li Peng, Si-Min Ma

School of Chemical Science and Technology, Key Laboratory of Medicinal Chemistry for Nature Resource, Ministry of Education, Yunnan University, Kunming, Yunnan, 650091, P. R. China

*E-mail: wanglin@ynu.edu.cn, wanglin2812@163.com

Received: 7 August 2016 / Accepted: 11 September 2016 / Published: 10 October 2016

The inhibition of mild steel corrosion in 1.0 mol/dm³ phosphoric acid (H₃PO₄) solution by methyl violet without and with bromide ion was studied using weight loss, potentiodynamic polarization and electrochemical impedance spectroscopy methods. The results indicate that combination of methyl violet and bromide ion performs excellent as inhibitor for mild steel corrosion in 1.0 mol/dm³ H₃PO₄ and a stronger synergistic effect exists between methyl violet and bromide ion. The electrochemical results indicate that single methyl violet or combination of bromide ion and methyl violet behaves as mixed type inhibitor with predominated of cathodic effect, and the corrosion reaction is controlled by charge transfer process. It is found that the adsorption process obeys Temkin adsorption isotherm in the absence of bromide ion and Langmuir adsorption isotherm in the presence of bromide ion, respectively. The thermodynamic and kinetic parameters (ΔG°_{ads} , ΔH°_{ads} , ΔS°_{ads} , K_{ads} and E_a) were calculated and discussed. The adsorption of inhibitor molecules on the steel surface is a spontaneous process containing physisorption and chemisorption. The outcomes from weight loss study are well in agreement with those obtained from electrochemical measurements.

Keywords: Corrosion inhibition, Mild steel; Phosphoric acid, Gravimetric methods, Electrochemical techniques, Adsorption, Thermodynamic properties..

1. INTRODUCTION

Acid solution is always easy to make corrosion of the metal. Sulphuric acid and hydrochloric acid are widely used in industrial applications such as acid pickling, removal undesirable rust, acid descaling, oil-well acidizing and acid cleaning [1]. Although phosphoric acid is a medium strong acid, it still shows stronger corrosiveness on ferrous or ferrous alloys [2-3]. As an important chemical product phosphoric acid has many applications especially in the production of fertilizers. In the wet

process of H_3PO_4 manufacture and the production of ammonium phosphate fertilizer, metallic materials are subject to the corrosion attack. Mild steel is widely used as constructional material in many industries because of its excellent mechanical properties and low cost [4]. One of the most effective methods in corrosion protection is the use of inhibitors [5-7]. Many organic compounds with heteroatoms such as nitrogen, oxygen, phosphorus and sulphur, π -electrons or aromatic rings are considered to be efficient corrosion inhibitors [8-20].

In general, inhibition of these compounds is attributed to the interaction between inhibitor molecules and steel surface by their adsorption on the metal surface, which means that the physical, chemical interaction or complexation can occur on a metal surface with inhibitor molecules [21-22]. The adsorption of inhibitor is affected by many factors such as nature of metals, the type of the aggressive environment and the structure of the inhibitor. Nitrogen-containing compounds were found to be more effective corrosion inhibitors for the steel in hydrochloric acid than in sulphuric acid [23-24]. The possible reason is that a synergistic inhibition may occur between nitrogen-containing organic inhibitors and chloride ions for steel in hydrochloric acid. Synergism is an effective method to improve the corrosion inhibition effect corresponding to the use of a single inhibitor and synergistic techniques have been applied in practice for its economy and efficiency [25-26].

Methyl violet (MV), an indicator in analytical chemistry, contains abundant π -electrons aromatic rings and nitrogen atoms unshared electron pairs. In a previous work, the corrosion inhibition of MV and chloride ion for the steel in sulphuric acid media was researched [27]. The results indicated that there was a good synergistic inhibition between chloride ion and MV for the steel corrosion. Chlorine and bromine are the adjacent elements of the same main group. Bromide ion should show the easier polarizability and better steric effect because the radius of bromide ion (Br^-) is bigger than that of chloride ion, which means that Br^- ions should be adsorbed on metal surface and provide better synergistic effect [24,28].

This investigation is to study the synergistic inhibition effect of Br^- and MV for mild steel corrosion in 1.0 mol/dm^3 H_3PO_4 media by weight loss, Tafel polarization and electrochemical impedance spectroscopy (EIS) methods. The adsorption behavior was described using the isotherm. The thermodynamic parameters were calculated and the adsorption mechanism was discussed. We hope to get some ideas to guide the composing of inhibitors in reality for H_3PO_4 system.

2. EXPERIMENTAL

2.1. Materials

The chemical composition of the mild steel used in this study was (wt%): 0.10% C, 0.017% S, 0.026% P, 0.050% Si, 0.28% Mn and Fe balance.

All solutions were prepared from bidistilled water and AR grade H_3PO_4 and potassium bromide (KBr) were used. Methyl violet was supplied by Merck Chemicals. The chemical structure of MV is presented in Figure 1.

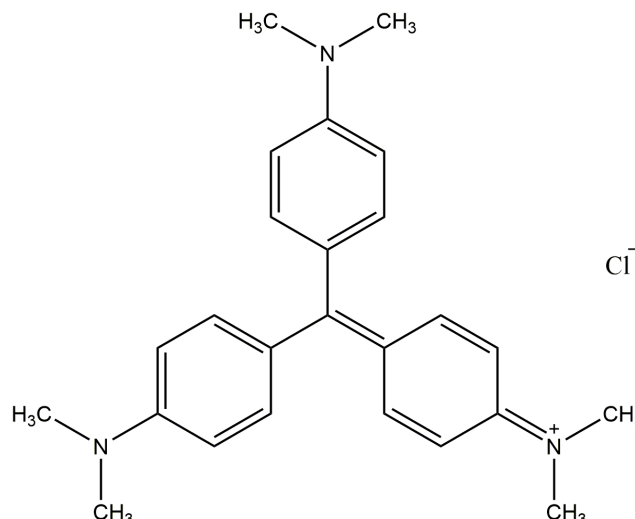


Figure 1. Structure of MV.

2.2. Weight loss measurements

The mild steel sheets (40 mm × 15 mm × 0.4 mm) were successively abraded with emery papers (grades 300, 600, 800, 1000 and 1200) until a mirror image was obtained. Then, the specimens were washed with distilled water, acetone and dried in a stream of air.

After weighing accurately, the specimens were immersed in testing solutions (150 ml) for 4 hours in air without bubbling. At the end of the run the specimens were taken out, washed, dried and immediately weighed accurately. Each measurement was performed on three separate samples and the average weight loss was taken.

2.3. Electrochemical measurements

The electrochemical cell consisted of a conventional three-electrode system with a working electrode, a reference electrode and an auxiliary electrode. The working electrodes were embedded in PVC holder using epoxy resin with an exposed area of 1.0 cm². Each working electrode was polished using emery papers (grades 300, 600, 800, 1000 and 1200) on the test face until a mirror image was obtained, washed with distilled water, acetone, and dried with a warm air stream. A platinum foil was considered as auxiliary electrode. The reference electrode was saturated calomel electrode (SCE) with Luggin capillary positioned very close to the surface of the working electrode in order to minimize ohmic potential drop. The working electrode was immersed in the testing solution at open circuit potential for two hours until a steady state potential was obtained before measurements.

PARSTAT 2263 Potentiostat/Galvanostat (Princeton Applied Research) was used for electrochemical measurements. The Tafel polarization curves were obtained on a scanning range of -250mV to +250mV around the open circuit potential, at a scanning rate of 0.5 mVs⁻¹. EIS measurements were performed in the frequency range of 100 kHz to 10 mHz using a 10 mV peak to peak voltage excitation. Each experiment was performed in triplicate to ensure reproducibility.

3. RESULTS AND DISCUSSION

3.1. Weight loss measurements

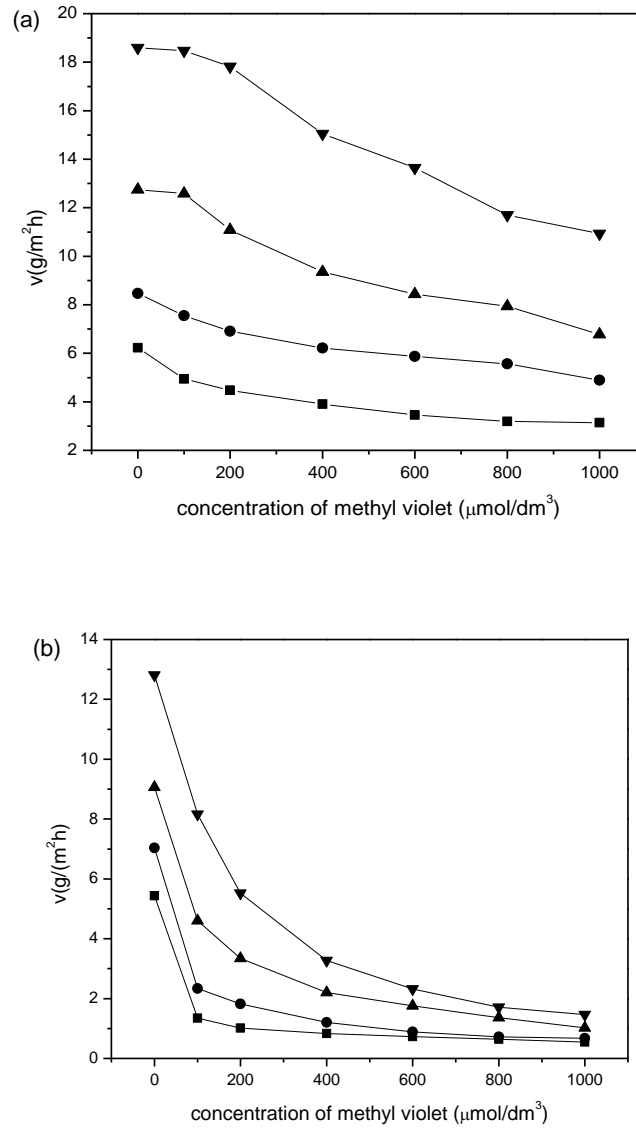


Figure 2. The corrosion rate curves of mild steel with different concentrations of MV in 1.0 mol/dm³ H₃PO₄ in the absence (a) and presence (b) of 0.05 mol/dm³ Br⁻. —■—25°C , —●—30 °C , —▲—35°C , —▼—40°C.

The inhibition efficiency (IE) was obtained from following formula [29]:

$$IE = \frac{V_0 - V_i}{V_0} \times 100 \quad (1)$$

where V_0 and V_i are the corrosion rates without and with the inhibitors, respectively. The corrosion rate changes of mild steel with different concentrations of MV without and with $0.05 \text{ mol/dm}^3 \text{ Br}^-$ in $1.0 \text{ mol/dm}^3 \text{ H}_3\text{PO}_4$ are given in Figure.2 at different temperatures.

It is seen from Figure 2(a), the corrosion rate of the steel decreases gradually with increasing MV concentration, while the corrosion rate increases as the temperature increases. Figure 2(b) gives the relationship of corrosion rate and MV concentration when $0.05 \text{ mol/dm}^3 \text{ Br}^-$ was added. Compared with Figure 2(a), it is clear that the corrosion rates drastically decrease with increase in the MV concentration in the presence of $0.05 \text{ mol/dm}^3 \text{ Br}^-$ for all the temperature ranges studied and the values of corrosion rate have not show obvious changes above $600 \text{ } \mu\text{mol/dm}^3 \text{ MV}$.

The inhibition efficiencies are given in Table 1 for single MV and combination of Br^- and MV in $1.0 \text{ mol/dm}^3 \text{ H}_3\text{PO}_4$ at experimental temperatures. As seen, the inhibition efficiencies increases gradually with increasing concentration of MV from 100 to $1000 \text{ } \mu\text{mol/dm}^3$ without Br^- , while the inhibition efficiencies decreases with increase in the temperature, which indicates the inhibition behaviour of MV against mild steel corrosion could be attributed to its adsorption on the steel surface. When the temperature increases, MV might be desorption from the steel surface because of reduction of surface coverage of MV on the mild steel surface and the steel surface exposed the acidic solution becomes less protected[30]. The highest inhibition efficiency is 49.5% (at $25 \text{ }^\circ\text{C}$) and the IE of single Br^- (0.05 mol/dm^3) also is not so well.

Table 1. Inhibition efficiencies for different concentrations of MV in the absence and presence of $0.05 \text{ mol/dm}^3 \text{ Br}^-$ in $1.0 \text{ mol/dm}^3 \text{ H}_3\text{PO}_4$ at experimental temperatures.

MV ($\mu\text{mol/dm}^3$)	Br^- (mol/dm^3)	Inhibition efficiency			
		25°C	30°C	35°C	40°C
0	0	—	—	—	—
100	0	20.6	10.8	1.25	0.52
200	0	28.1	18.4	13.0	4.13
400	0	37.2	26.6	24.6	19.0
600	0	44.4	33.8	30.6	26.6
800	0	48.7	37.7	36.3	34.1
1000	0	49.5	46.8	42.2	41.2
0	0.05	12.7	16.9	28.9	31.1
100	0.05	78.4	72.4	63.9	56.1
200	0.05	83.7	78.5	73.8	70.3
400	0.05	86.7	85.8	82.7	82.4
600	0.05	89.3	88.5	87.5	87.1
800	0.05	90.3	90.8	90.1	90.0
1000	0.05	92.2	92.0	92.0	91.8

In the presence $0.05 \text{ mol/dm}^3 \text{ Br}^-$ it is quite obvious that the inhibition efficiencies are greatly enhanced compared with those only in the presence of single Br^- or MV. For instance, the inhibition

efficiency is over 90% at 800 $\mu\text{mol}/\text{dm}^3$ MV, which indicates that the combination of Br^- and MV is a highly efficient inhibitor of the mild steel corrosion in 1.0 mol/dm^3 H_3PO_4 media.

3.2. Adsorption isotherm

The adsorption process can be described according to adsorption isotherms because they can provide valuable information on the interaction of the inhibitor with the metal surface. In order to obtain the adsorption isotherm, the degree of surface coverage (θ) was calculated using the following equation [31]:

$$\theta = \frac{V_0 - V}{V_0 - V_m} \quad (2)$$

where V is the corrosion rate with addition of inhibitor and V_m is the smallest corrosion rate.

It was found that in the absence of Br^- , the adsorption of MV on the mild steel surface in 1.0 mol/dm^3 H_3PO_4 was fitted to Temkin adsorption isotherm, as follow:

$$\exp(-2a\theta) = K_{ads} C \quad (3)$$

Where K_{ads} is the adsorptive equilibrium constant, C is the concentration of the inhibitor and a is the lateral interaction term describing the molecular interactions in the adsorption layer and the heterogeneity of the metal surface. Eq. (3) can be transformed into another kind of expression form:

$$\theta = \frac{\ln K_{ads}}{-2a} + \frac{\ln c}{-2a} \quad (4)$$

According to the Eq.4, the linear regression between θ and $\ln C$ were shown in Figure 3 and the corresponding parameters calculated are given in Table 2 in the absence of 0.05 mol/dm^3 Br^- .

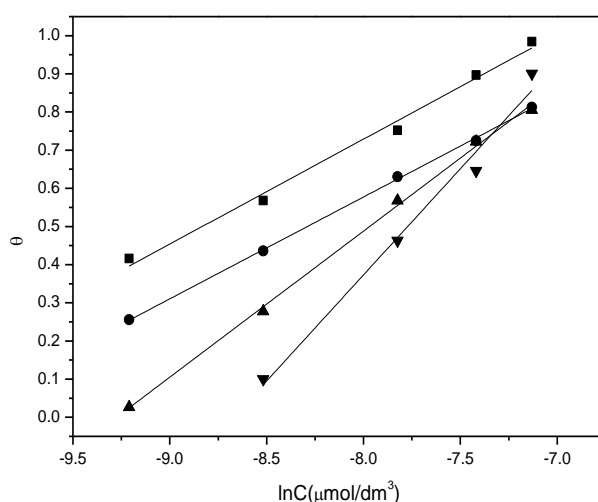


Figure 3. The relationship between θ and $\ln C$ in the absence of Br^- in 1.0 mol/dm^3 H_3PO_4 . —■—25 °C , —●—30°C , —▲—35°C , —▼—40°C.

It can be seen from Table 2 that the linear correlation coefficients are almost close to 1, meaning the adsorption follows the Temkin adsorption isotherm. It is also found that the values of K_{ads} are larger to 10^4 , which shows the adsorption trend of MV on the mild steel surface is stronger. However the values of α are < 0 , meaning that the repulsion exists in the adsorption layer.

With addition of $0.05 \text{ mol/dm}^3 \text{ Br}^-$, the adsorption of MV on the steel surface obeys the Langmuir adsorption isotherm where:

$$\frac{C}{\theta} = \frac{1}{K_{ads}} + C \quad (5)$$

The relationship between C and C/θ without $0.05 \text{ mol/dm}^3 \text{ Br}^-$ is given in Figure 4 and the corresponding parameters obtained are also listed in Table 3.

Table 2. Parameters of the linear regression between θ and $\ln C$ in the absence of Br^- .

Temperature (°C)	Linear regression coefficient	α	K_{ads} ($\times 10^4 \text{ dm}^3/\text{mol}$)
25	0.9960	-1.818	4.222
30	0.9997	-1.873	2.595
35	0.9992	-1.306	1.066
40	0.9929	-0.899	0.583

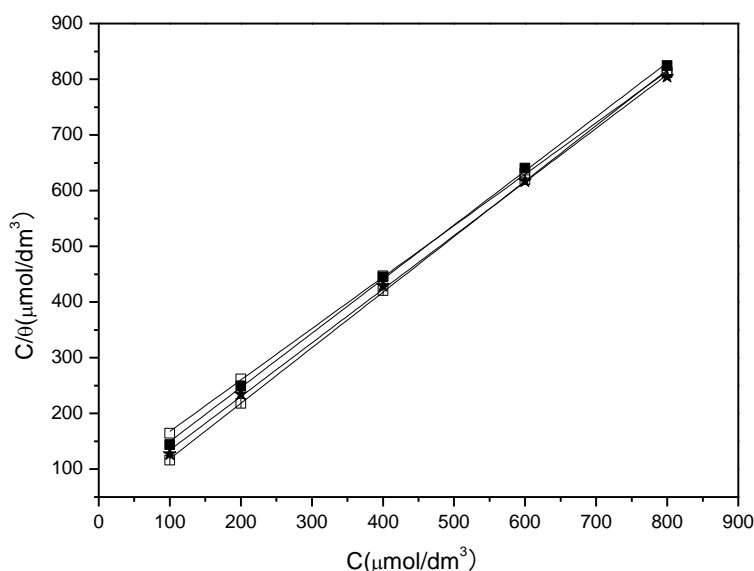


Figure 4. The relationship between C and C/θ in the presence of $0.05 \text{ mol/dm}^3 \text{ Br}^-$ in $1.0 \text{ mol/dm}^3 \text{ H}_3\text{PO}_4$. —□— 25°C , —■— 30°C , —★— 35°C , —◇— 40°C .

Compared the values of K_{ads} obtained without and with $0.05 \text{ mol/dm}^3 \text{ Br}^-$, it is clear that the values of K_{ads} are larger with Br^- than without Br^- , meaning that the adsorption trend of mixture of MV and Br^- is stronger than single MV on the surface of mild steel.

Table 3. Parameters of the linear regression between C/θ and C in the presence of $0.05 \text{ mol/dm}^3 \text{ Br}^-$.

Temperature (°C)	Linear regression coefficient	slope	K_{ads} ($\times 10^4 \text{ dm}^3/\text{mol}$)
25	0.9999	0.9971	5.308
30	0.9998	0.9630	2.643
35	0.9998	0.9715	1.903
40	0.9999	0.9235	1.326

3.3. Thermodynamic parameters

From the thermodynamic model, the adsorption phenomenon of inhibitor and the corrosion inhibition of mild steel can be better explained using some thermodynamic parameters. From the Van't Hoff formula [32]:

$$\ln K_{ads} = \frac{-\Delta H_{ads}^{\circ}}{RT} + B \quad (6)$$

where R is the universal gas constant, T is the absolute temperature, ΔH_{ads}° is the standard adsorption heat and B is a constant. It can be seen that the adsorption heat can be counted according to the slope of the regression.

Table 4. The thermodynamic data for mild steel corrosion in $1.0 \text{ mol/dm}^3 \text{ H}_3\text{PO}_4$ containing MV and Br^- at experimental temperatures.

Temperature (°C)	Br^- (mol/dm^3)	ΔG_{ads}° (kJ/mol)	ΔH_{ads}° (kJ/mol)	ΔS_{ads}° (J/mol K)
25	0	-36.36	-105.7	-232.6
30	0	-35.74	-105.7	-230.8
35	0	-34.05	-105.7	-232.5
40	0	-33.03	-105.7	-232.1
25	0.05	-36.92	-69.63	-109.7
30	0.05	-35.79	-69.63	-111.6
35	0.05	-35.53	-69.63	-110.7
40	0.05	-35.17	-69.63	-110.0

The standard free energy of adsorption (ΔG_{ads}°) can be obtained according to equation (7) [33-34]:

$$K_{ads} = \frac{1}{55.5} \exp\left(\frac{-\Delta G_{ads}^{\circ}}{RT}\right) \quad (7)$$

where the number 55.5 is the molar concentration of water. Then the standard adsorption (ΔS_{ads}°) can be calculated based on the thermodynamic basic equation:

$$\Delta G_{ads}^{\circ} = \Delta H_{ads}^{\circ} - T\Delta S_{ads}^{\circ} \quad (8)$$

Table 4 gives the thermodynamic parameters obtained.

Normally, the values of ΔG_{ads}° around -20 kJ/mol or less negative are assigned for the electrostatic interactions exist between inhibitor and the charged metal surface (physisorption). Meanwhile, higher $-\Delta G_{ads}^{\circ}$ values than -40 kJ/mol are consistent with chemisorption, meaning that the electrons might share or transfer from the inhibitor molecules to the metal surface to form a coordinate type of metal bond [35-36].

The negative values of ΔG_{ads}° indicate spontaneous adsorption process of the inhibitor molecules on the mild steel surface in 1.0 mol/dm³ H₃PO₄ solution with and without Br⁻. These values are found to be between -33.03 and -36.92 kJ/mol, indicating that adsorption mechanism of the inhibitor molecules on the mild steel is a combination of both physisorption and chemisorption [18]. The physisorption could occur between the active positive centers on the metal surface and π -bonds in the benzene ring of MV or Br⁻, while the chemisorption is the formation of coordinated bond between the inhibitor molecules and the d-orbital of iron on steel surface through π -electrons or lone pair of electron of N atoms of MV [37-38]

In the absence and presence of Br⁻, the negative values of ΔH_{ads}° means that the adsorption of MV or combination of Br⁻ and MV on the steel surface is an exothermic process. The negative values of ΔS_{ads}° indicates that the adsorption is a process of entropy decrease, which could be explained by the following: The inhibitors molecules could be chaotic and free moving in the bulk solution before the adsorption of inhibitor molecules on the steel surface took place. With the progress in the adsorption, inhibitor molecules were orderly adsorbed on the steel surface accompanied by decrease in disordering, as a result, a decrease in entropy [39-40]. The negative enthalpy and negative entropy indicates that the exothermic is the principal determinant of spontaneous adsorption of MV and Br⁻ on the surface of mild steel in 1.0 mol/dm³ H₃PO₄.

3.4. Effect of temperature

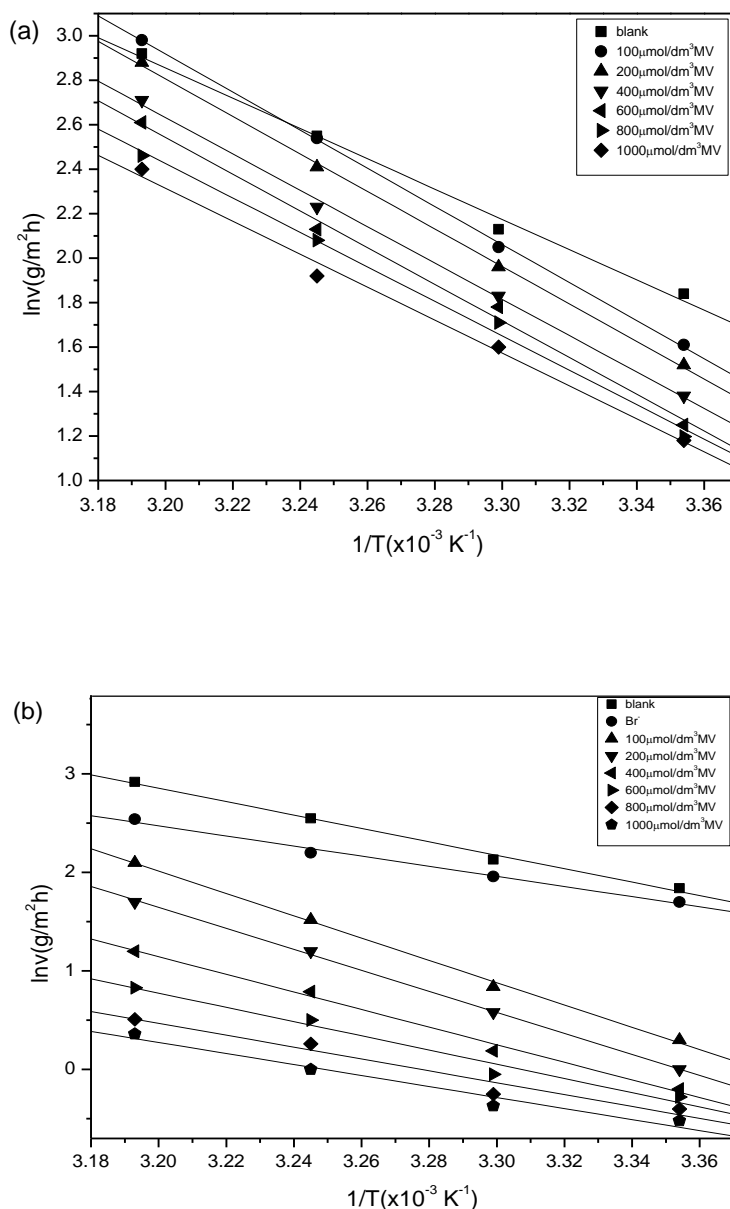


Figure 5. Arrhenius plots of mild steel in 1.0 mol/dm³ H₃PO₄ in the absence (a) and presence (b) of 0.05 mol/dm³ Br⁻.

Table 5. Parameters of the linear regression between lnV and 1/T.

MV (μmol/dm ³)	Br ⁻ (mol/dm ³)	E _a (kJ/mol)	Pre-exponential factor A (g/m ² h)	Linear regression coefficient
0	0	56.63	5.078×10 ¹⁰	0.9970
100	0	71.21	1.481×10 ¹³	0.9997
200	0	70.11	8.670×10 ¹²	0.9996
400	0	67.94	3.160×10 ¹²	0.9991

600	0	68.59	3.709×10^{12}	0.9974
800	0	64.39	6.547×10^{11}	0.9976
1000	0	61.58	1.985×10^{11}	0.9967
0	0.05	42.69	1.620×10^8	0.9960
100	0.05	94.11	4.028×10^{16}	0.9989
200	0.05	88.58	3.326×10^{15}	0.9995
400	0.05	74.31	8.828×10^{12}	0.9965
600	0.05	60.03	2.354×10^{10}	0.9883
800	0.05	50.13	3.838×10^8	0.9794
1000	0.05	46.51	7.829×10^7	0.9834

Temperature plays an important role on the progress of the corrosion reactions of mild steel in H_3PO_4 solution. The mechanism of the inhibitors action can be further elucidated by kinetic model. The activation parameters for the corrosion process were calculated from Arrhenius Equation:

$$\ln V = \frac{-E_a}{RT} + \ln A \quad (9)$$

where E_a is apparent activation energy and A is pre-exponential factor. The Arrhenius plots of $\ln V$ vs. $1/T$ is shown in Figure 5 in the absence (a) and presence (b) of Br^- , respectively.

The values E_a and A were obtained by the slopes and intercepts of the Arrhenius plots, respectively, listed in Table 5. In the absence of Br^- the activation energies for inhibited solution were larger than that for the blank solution, which indicated the presence of energy barrier on the surface of mild steel [41]. In the presence of Br^- , only at higher concentrations of MV (800-1000 mol/dm³) the activation energies are lower than that of the blank.

From Eq.7, it is clear that the corrosion rate of mild steel is controlled by the apparent activation energy and pre-exponential factor at a certain temperature. In the absence of Br^- , the decrease of mild steel corrosion rate is mainly controlled depending on the increase of the E_a . In the presence of Br^- , the decrease of the corrosion rate is also determined by the increase of the E_a between the 100 – 600 $\mu\text{mol/dm}^3$ MV. When the MV concentration is above 800 $\mu\text{mol/dm}^3$, the reduction of the pre-exponential factor decides the decrease of the corrosion rate.

3.5. Polarization measurements

Anodic and cathodic polarization plots of mild steel with different concentrations of MV in the absence and presence of 0.05 mol/dm³ Br^- in 1.0 mol/dm³ H_3PO_4 at 25 °C are presented in Figure 6. It can be seen from Figure 6 (a), MV slightly shifted the corrosion potential (E_{corr}) in the negative direction and some retardation of the anodic reaction was observed but cathodic polarization was dominant in the absence of Br^- .

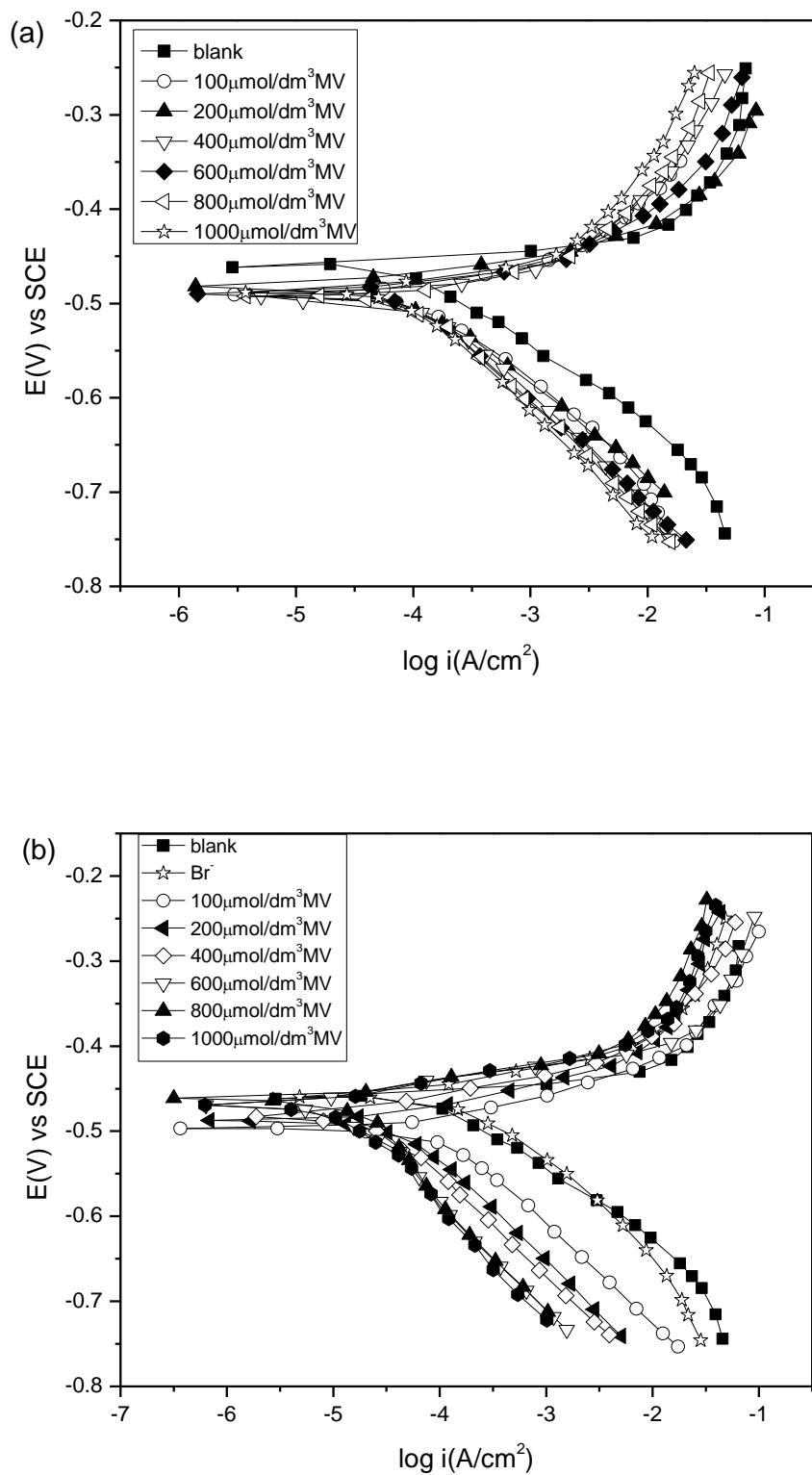


Figure 6. Tafel polarization curves of mild steel containing different concentrations of MV in the absence (a) and presence (b) 0.05 mol/dm³ Br⁻ in the 1.0 mol/dm³ H₃PO₄ at 25 °C.

From Figure 6 (b), with addition of 0.05 mol/dm³ Br⁻, combination of Br⁻ and MV slightly shifted E_{corr} to both negative and positive directions and retardation of the cathodic reaction was still dominant. Compared with Figure 6 (a), the shifting levels were obviously larger mixture of MV and Br⁻ than single MV. These results show that the single MV or combination of Br⁻ and MV in 1.0 mol/dm³ H₃PO₄ acted as a mixed-type inhibitor but cathodic polarization was dominant for the mild steel corrosion.

The inhibition efficiency values were obtained according to the following formula [42]:

$$IE = \frac{I_{\text{corr}}^0 - I_{\text{corr}}^{\text{inh}}}{I_{\text{corr}}^0} \times 100 \quad (10)$$

where I_{corr}^0 and $I_{\text{corr}}^{\text{inh}}$ are the corrosion current density values without and with inhibitors.

The electrochemical polarization parameters: corrosion current density (I_{corr}), corrosion potential (E_{corr}), cathodic and anodic Tafel slopes (β_c , β_a) of the corrosion process are given in Table 6.

There is no regular change in Tafel slopes with changing the inhibitor concentrations, this feature means that the anodic steel dissolution and cathodic hydrogen evolution reactions were both inhibited by the inhibitors through merely blocking the reaction active centers of mild steel surface without affecting the cathodic and anodic reaction mechanism [43-44].

Comparing the values of corrosion current densities and IE in the presence of Br⁻ with those in the absence of Br⁻, declines of I_{corr} and improvements of IE could be seen clearly in the presence of Br⁻, also showing that combination of Br⁻ and MV is a highly efficient inhibitor of the mild steel corrosion in 1.0 mol/dm³ H₃PO₄ media.

Table 6. Electrochemical polarization data for mild steel corrosion in 1.0 mol/dm³ H₃PO₄ containing MV and Br⁻ at 25 °C.

MV ($\mu\text{mol}/\text{dm}^3$)	Br ⁻ (mol/dm^3)	E_{corr} (vs. SCE) (mV)	I_{corr} ($\mu\text{A}/\text{cm}^2$)	$-\beta_c$ (mV/dec)	β_a (mV/dec)	IE
0	0	-463.6	232.7	98.16	61.39	—
100	0	-489.3	193.9	111.6	52.13	16.7
200	0	-481.7	153.9	124.7	51.03	33.9
400	0	-491.1	148.2	109.9	30.23	36.3
600	0	-490.6	133.0	112.5	36.71	42.8
800	0	-490.3	125.9	114.8	31.51	45.9
1000	0	-485.1	110.7	121.1	28.22	52.4
0	0.05	-457.1	183.6	112.0	53.26	21.1
100	0.05	-496.0	101.9	114.8	43.08	56.2
200	0.05	-494.1	59.63	128.2	55.09	74.4
400	0.05	-494.2	36.66	121.6	46.33	84.3
600	0.05	-459.6	18.85	141.0	23.10	91.9
800	0.05	-457.4	16.99	134.8	21.71	92.7
1000	0.05	-466.0	15.82	132.6	25.73	93.2

3.6. Electrochemical impedance spectroscopy

Nyquist plots of mild steel with different concentrations of MV in the absence and presence of $0.05 \text{ mol/dm}^3 \text{ Br}^-$ in $1.0 \text{ mol/dm}^3 \text{ H}_3\text{PO}_4$ at 25°C are presented in Figure 7.

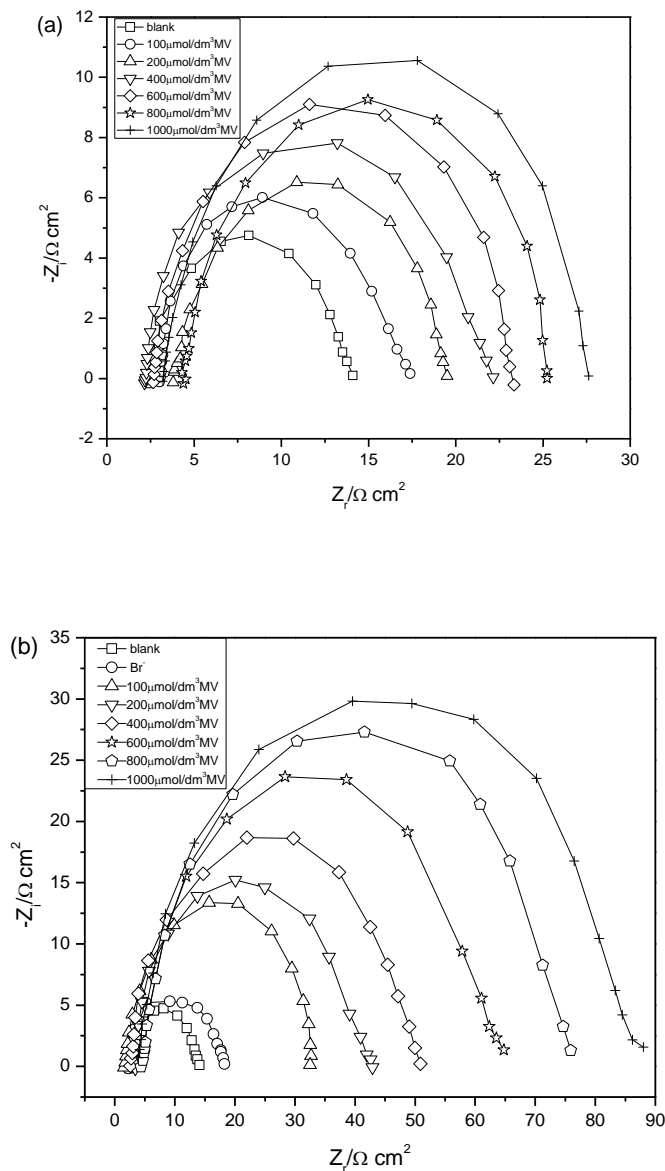


Figure 7. Nyquist plots of mild steel containing different concentrations of MV in the absence (a) and presence (b) $0.05 \text{ mol/dm}^3 \text{ Br}^-$ in $1.0 \text{ mol/dm}^3 \text{ H}_3\text{PO}_4$ at 25°C .

All the Nyquist plots display a single capacitive loop of characteristic depressed semicircles in the absence and presence of inhibitors in H_3PO_4 , which means that the charge transfer controls occurrence of corrosion process. The charge-transfer process influenced predominantly inhibition of mild steel corrosion and the mechanism of mild steel dissolution was not modified with the addition of the inhibitor [45]. The capacitive loops are imperfect semicircles which is related to the frequency dispersion effect due to the roughness and inhomogeneous of the electrode surface [46]. Comparing

the semicircles in the presence of Br⁻ with those in the absence of Br⁻, the diameters of the capacitance loops are clearly bigger in the presence of Br⁻ than in the absence of Br⁻, suggesting that the presence of Br⁻ can enhance anti-corrosion performance of MV effectively.

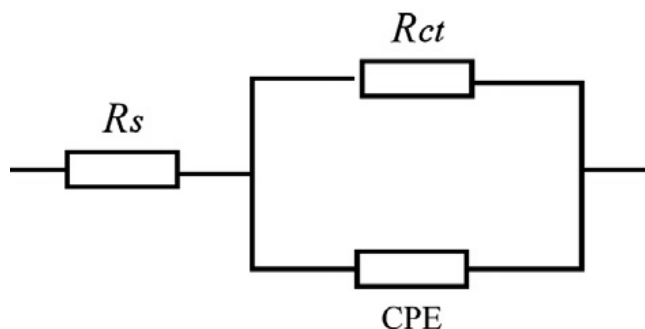


Figure 8. The equivalent electric circuit used to obtain the impedance parameters.

The impedance data of mild steel in 1.0 mol.dm³ H₃PO₄ are analyzed in terms of an equivalent circuit model which is well-known Randle cell, as given in Figure 8, which includes solution resistance (R_s), charge transfer resistance (R_{ct}) and a constant phase element (CPE). The double layer capacitance (C_{dl}) value affected by imperfections of the surface is simulated via CPE [47]. The CPE is composed of a component Q_{dl} and a coefficient b which quantifies different physical phenomena such as inhibitor adsorption, porous layer formation, surface inhomogeneous resulting from surface roughness, etc. The C_{dl} can be calculated as follows [23]:

$$C_{dl} = Q_{dl} \cdot (2\pi f_{max})^{b-1} \quad (11)$$

where f_{max} represents the frequency at which the imaginary value reaches a maximum on the Nyquist plot.

The inhibition efficiencies could be calculated using the following formula:

$$IE_t = \frac{R_{ct(inh)} - R_{ct(0)}}{R_{ct(inh)}} \times 100 \quad (12)$$

where $R_{ct(0)}$ and $R_{ct(inh)}$ are the charge-transfer resistances in the absence and presence of inhibitor, respectively. The values of R_{ct} , C_{dl} , R_s , and IE_{ct} are shown in Table 7.

From Table 7, the values of C_{dl} is decrease in the presence of inhibitors compare to the blank solution, meaning that the increase in the thickness of the electrical double layer may be responsible for this decrease in C_{dl} , which suggests the adsorption of inhibitor molecules at the metal/solution interface [48]. At the same time, the values of R_{ct} increase with increasing MV concentration denoting increase in the inhibition efficiencies no matter without or with Br⁻. But the increase of R_{ct} or IE_{ct} is clearly larger with Br⁻ than without Br⁻. These results are well in accordance with those acquired by polarization measurements and weight loss.

Table 7. Electrochemical impedance data for mild steel corrosion in 1.0 mol/dm³ H₃PO₄ containing MV and Br⁻ at 25 °C.

MV	Br ⁻	R_s	C_{dl}	R_{ct}	IE_{ct}
----	-----------------	-------	----------	----------	-----------

($\mu\text{mol}/\text{dm}^3$)	(mol/dm^3)	($\Omega \text{ cm}^2$)	($\mu\text{F}/\text{cm}^2$)	($\Omega \text{ cm}^2$)	
0	0	2.595	154.2	11.33	
100	0	2.991	108.5	14.73	23.1
200	0	4.012	100.5	15.53	27.0
400	0	2.191	87.53	18.60	39.1
600	0	2.761	76.11	20.52	44.8
800	0	5.516	74.81	21.09	46.3
1000	0	3.302	66.36	24.71	54.2
0	0.05	2.601	116.2	13.99	19.0
100	0.05	2.044	63.26	30.91	63.3
200	0.05	2.780	57.19	39.07	71.0
400	0.05	3.377	46.76	47.61	76.2
600	0.05	2.795	35.64	60.26	81.2
800	0.05	4.502	32.63	70.37	83.9
1000	0.05	3.892	26.15	83.31	86.4

3.7. Synergism parameters

The above studies indicate that there may be a synergistic inhibition action of Br^- and MV for mild steel corrosion in $1.0 \text{ mol}/\text{dm}^3 \text{ H}_3\text{PO}_4$, which can be examined using synergism parameters (S), calculated as follows [45]:

$$S = \frac{1 - (IE_1 + IE_2)}{1 - IE_{1+2}} \quad (13)$$

where IE_1 is the inhibition efficiency of inhibitor 1 and IE_2 is the inhibition efficiency of inhibitor 2, IE_{1+2} is the inhibition efficiency in coexistence of the both inhibitors.

Table 8. Synergism parameters of Br^- and MV for corrosion inhibition of mild steel in $1.0 \text{ mol}/\text{dm}^3 \text{ H}_3\text{PO}_4$ at experimental temperatures.

MV ($\mu\text{mol}/\text{dm}^3$)	Br^- (mol/dm^3)	Synergism parameters(S)			
		25°C	30°C	35°C	40°C
100	0.05	3.088	2.620	1.935	1.588
200	0.05	3.632	3.009	2.218	2.181
400	0.05	3.768	3.979	2.688	2.835
600	0.05	4.009	4.287	3.240	3.279
800	0.05	3.979	4.935	3.515	3.480
1000	0.05	4.846	4.538	3.613	3.378

Generally, when value of S is < 1 , meaning that antagonistic behavior leading to competitive adsorption prevails, whereas $S > 1$ shows that there is a synergistic action [49].

The S values obtained are listed in Table 8. It is clear that all of S values are greater than 1 and behave quite large, which indicates that the combination Br^- and MV expresses a stronger synergistic inhibition action for mild steel in $1.0 \text{ mol/dm}^3 \text{ H}_3\text{PO}_4$, and inhibition efficiency gets greatly improved.

In acid solution, steel surface contains positive charge due to $E_{\text{corr}} - E_{q=0}$ (zero charge potential) > 0 [50], and MV could be protonated as to $[\text{MVH}_x]^{x+}$. The positively charged MV can hardly approach the positively charged surface of steel directly because of the electrostatic repulsion. With addition of Br^- , bromide ions can be specifically adsorbed on the steel surface charged positively. In this way, potential of zero charge becomes less negative which promotes the adsorption of inhibitors in cationic form [34,51]. The adsorption of MV molecules can occur through donor-acceptor interactions between the abundance π -electrons or nitrogen atom in MV and the unoccupied d-orbital of the iron atoms. As a result, physisorption and chemisorption may be acting on the mild steel surface.

4. CONCLUSION

(1) Single MV or Br^- has not satisfactory inhibition efficiency for mild steel in $1.0 \text{ mol/dm}^3 \text{ H}_3\text{PO}_4$. With the addition of $0.05 \text{ mol/dm}^3 \text{ Br}^-$, the inhibition efficiency of MV is greatly enhanced. The synergism parameters suggest that a stronger synergistic inhibition action exists between Br^- and MV in H_3PO_4 for mild steel corrosion.

(2) In the absence of Br^- the adsorption of MV on steel surface obeys the Temkin adsorption isotherm. However the adsorption of MV obeys the Langmuir adsorption isotherm in the presence of Br^- . The adsorption of inhibitor molecules on the steel surface is a spontaneous process containing physisorption and chemisorption.

(3) Single MV or combination of Br^- and MV retards the anodic and cathodic corrosion reaction but cathodic polarization is dominant for steel corrosion in $1.0 \text{ mol/dm}^3 \text{ H}_3\text{PO}_4$, They behave as mixed type inhibitors reducing the steel dissolution and retarding hydrogen evolution reactions by blocking the active reaction centers on the mild steel surface.

(4) EIS indicates that occurrence of corrosion process is controlled by charge transfer.

The results obtained from weight loss, polarization measurements and electrochemical impedance spectroscopy are concordant.

ACKNOWLEDGEMENT

This work was financially supported by the National Natural Science Foundation of China under the Grant No. 51161025

References

1. K.C. Emregül and M. Hayvalı, *Corros. Sci.*, 48 (2006) 797.
2. P.B. Mathur and T. Vasudevan, *Corrosion* 38 (1982) 171.

3. L. Wang, *Corros. Sci.*, 48 (2006) 608.
4. N.S. Ayati, S. Khandandel, M. Momeni, M.H. Moayed, A. Davoodi and M. Rahimizadeh, *Mater. Chem. Phys.* 126 (2011) 873.
5. M. Farsak, H. Keleş and M. Keleş, *Corros. Sci.*, 98 (2015) 223.
6. A. Ganash, *Int. J. Electrochem. Sci.*, 10 (2015) 4439.
7. R. Solmaz, G. Kardaş, M. Çulha, B. Yazıcı and M. Erbil, *Electrochim. Acta* 53 (2008) 5941.
8. P. Thanapackiam, S. Rameshkumar, S.S. Subramanian and K. Mallaiya, *Mater. Chem. Phys.*, 174 (2016) 129.
9. C. Cardona, A.A. Torres, J.M. Miranda-Vidales, J.T. Pérez, M.M. González- Chávez, H. Herrera-Hernández and L.Narváez, *Int. J. Electrochem. Sci.*, 10 (2015) 1966.
10. G. Žerjav and I. Milošev, *Corros. Sci.*, 98 (2015) 180.
11. A. Aytaç, S. Bilgiç, G. Gece, N. Ancin and S.G. Öztaş, *Mater. Corros.*, 63 (2012) 729.
12. L. Wang, J.X. Pu and H.C. Luo, *Corros. Sci.*, 45 (2003) 677.
13. L.A. Al Juhaiman, *Int. J. Electrochem. Sci.*, 11 (2016) 2247.
14. L. Afia, R.Salghi, O.Benali, S.Jodeh, I.Warad, E. Ebenso and Hammouti, *Electrochim. Acta*, 33 (2015) 137.
15. S.K. Shukla and E.E. Ebenso, *Int. J. Electrochem. Sci.*, 6 (2011) 3277.
16. R.Y. Khaled, A.M. Abdel-Gaber and H.M. Holail, *Int. J. Electrochem. Sci.*, 11 (2016) 2790.
17. M.A. Hegazy, A.M. Badawi, S.S. Abd El Rehim and W.M. Kamel, *Corros. Sci.*, 69 (2013) 110.
18. A.Y. Musa, A.B. Mohamad, A.A.H. Kadhum and M.S. Takriff, *Int. J. Electrochem. Sci.*, 6 (2011) 2758.
19. A. M. Al-Bonayan, *Int. J. Electrochem. Sci.*, 10 (2015) 589.
20. Sh. Pournazari, M.H. Moayed and M. Rahimizadeh, *Corros. Sci.*, 71 (2013) 20.
21. G. Quartarone, L. Banaldo and C. Tartato, *Appl. Surf. Sci.*, 252 (2006) 8251.
22. I. Lukovits, E. Kálmán and F. Zucchi, *Corrosion*, 57 (2001) 3.
23. M. Lagrenée, B. Mernari, M. Bouanis, M. Traisnel and F. Bentiss, *Corros. Sci.*, 44 (2002) 573.
24. R. Fuchs-Godec and M.G. Pavlović, *Corros. Sci.*, 58 (2012) 192.
25. I.B. Obot, N.O. Obi-Egbedi and S.A. Umoren, *Corros. Sci.*, 51 (2009) 276.
26. H. Amar, J. Benzakour, A. Derja, D. Villemin and B. Moreau, *Corros. Sci.*, 50 (2008) 124.
27. L. Wang, F. Yang, J. Ma, Z. Fang, S. Zhang, Q. Guo, *Asian J. Chem.*, 25 (2013) 10305.
28. G.K. Gomma, *Mater. Chem. Phys.*, 55 (1998) 241.
29. ASTM G1-72, Practice for preparing, cleaning and evaluating corrosion test specimens (1990).
30. E.E Ebenso, I.B. Obot, *Int. J. Electrochem. Sci.* 5 (2010) 2012.
31. I. Sekine, Y. Hirakawa, *Corrosion*, 42 (1986) 272.
32. L. Wang, S.W. Zhang, Q. Guo, H. Zheng, D.M. Lu, L. Peng and J Xion, *Mater. Corros.*, 66 (2015) 594
33. M. Lebrini, M. Lagrenée, M. Traisnel, L. Genembre, H. Vezin and F. Bentiss, *Appl. Surf. Sci.*, 253 (2007) 9267.
34. S.K. Shukla and M.A. Quraishi, *Corros. Sci.*, 51 (2009) 1007.
35. E. Machnikova, K.H. Whitmire and N. Hackerman, *Electrochim. Acta* 53 (2008) 6024
36. G. Moretti, F Guidi, and G. Grion, *Corros. Sci.*, 46 (2004) 387.
37. M.A. Hegazy and M.F. Zaky, *Corros. Sci.*, 52 (2010) 1333.
38. J. Flis, T. Zakroczymski, *J. Electrochem. Soc.*, 143 (1996) 2458.
39. I.B. Obot and N.O. Obi-Egbedi, *Colloids Surf. A*, 330 (2008) 207.
40. N.O. Eddy and E.E Ebenso, *Afr. J. Pure Appl. Chem.*, 2(2008) 46.
41. I.N. Putilova, V.P. Barannik and S.S. Balezin, *Metallic Corrosion Inhibitors*, Pregamon press, Oxford,30 (1960) 32.
42. S.A. Abd El-Maksoud and A.S. Fouda, *Mater. Chem. Phys.*, 93 (2005) 84.
43. A.K. Satapathy, G. Gunasekaran, S.C. Sahoo, K. Amit and P.V. Rodrigues, *Corros. Sci.*, 51 (2009) 2848.

44. K. C. Emeregül, M. Hayvalı, *Corros. Sci.*, 48 (2006) 797.
45. L. Larabi, Y. Harek, M. Traisnel and A. Mansri, *J. Appl. Electrochem.*, 34 (2004) 833.
46. M. Lebrini, M. Lagrenée, H. Vezin, M. Traisnel and F. Bentiss, *Corros. Sci.*, 49 (2007) 2254.
47. P. Bommersbach, C. Alemany-Dumont, J. P. Millet, B. Normand, *Electrochim. Acta*, 51 (2006) 4011.
48. M. Behpour, S.M. Ghoreishi, M. Khayatkashani and N. Soltani, *Corros. Sci.*, 53 (2011) 2489.
49. S. A. Umeron, O. Ogbobe, I. O. Igwe, E. E. Ebenso, *Corros. Sci.*, 50 (2008) 1998.
50. Ali Döner, E.A. Şuhin, G. Kardaş and O. Serindağ, *Corros. Sci.*, 66 (2013) 278.
51. H. Ashassi-Sorkabi, N. Gahlebsaz-Jeddi, F. Hashemzadeh and H.jahani, *Electrochim. Acta*, 51 (2006) 3848.

© 2016 The Authors. Published by ESG (www.electrochemsci.org). This article is an open access article distributed under the terms and conditions of the Creative Commons Attribution license (<http://creativecommons.org/licenses/by/4.0/>).